Talanta 85 (2011) 575–581

Contents lists available at ScienceDirect

Talanta

journal homepage: www.elsevier.com/locate/talanta

Stabilization of sensing performance for mixed-potential-type zirconia-based hydrocarbon sensor

Yuki Fujio[a,b], Vladimir V. Plashnitsa[c], Perumal Elumalai[d,1], Norio Miura[d,*]

[a] Interdisciplinary Graduate School of Engineering Sciences, Kyushu University Kasuga-shi, Fukuoka 816-8580, Japan
[b] Japan Society for the Promotion of Science, Tokyo 102-8471, Japan
[c] Research and Education Center of Carbon Resources, Kyushu University, Kasuga-shi, Fukuoka 816-8580, Japan
[d] Art, Science and Technology Center for Cooperative Research, Kyushu University, Kasuga-shi, Fukuoka 816-8580, Japan

ARTICLE INFO

Article history:
Received 18 January 2011
Received in revised form 11 April 2011
Accepted 11 April 2011
Available online 16 April 2011

Keywords:
Mixed-potential
Gas sensor
YSZ
Hydrocarbons
$ZnCr_2O_4$

ABSTRACT

The recently reported sensing characteristics of the mixed-potential-type yttria-stabilized zirconia (YSZ)-based hydrocarbon (HC) sensor attached with $ZnCr_2O_4$-sensing electrode (SE) were found to be changed after the 10-day operation at 550 °C under the wet condition (5 vol.% water vapor). To improve the stability of the present sensor, the several modifications of the SE material by adding YSZ powder were examined. As a result, the sensor using the laminated ($ZnCr_2O_4$/YSZ)-SE gave the stable electromotive force (*emf*) response against 100 ppm C_3H_6 at 550 °C for about one month examined. Based on the scanning electron microscopy (SEM) observation and the AC complex-impedance measurements, it was concluded that the stable behavior of the sensor using the laminated ($ZnCr_2O_4$/YSZ)-SE was provided by the stabilization of the interface between $ZnCr_2O_4$ grains and YSZ particles. The fabricated sensor exhibited the linear dependence of sensitivity on the logarithm of either C_3H_6 concentration (in the range of 20–800 ppm) or mixtures of various hydrocarbons (HCs) (in the range of 90–2600 ppmC). In addition, the *emf* response was not altered by the change of O_2 (2–20 vol.%), H_2O (0–10.8 vol.%) and CO_2 (0–20 vol.%) concentrations, and no interference of other gases (CO, NO, NO_2, H_2, and CH_4) was observed.

© 2011 Elsevier B.V. All rights reserved.

1. Introduction

For a last few decades, the number of automobiles has been drastically increasing. As a consequence, the emission control for automobiles containing the gasoline and diesel engines have been severely regulated all around the world, especially in USA, Japan and European Union. Among the various air pollutants such as CO, NO_x (NO and NO_2) and hydrocarbons (HCs), some of HCs cause a photochemical smog or greenhouse effect, affecting an environmental eco-system. Thus, to control an efficiency of conventional post-engine treatment systems (e.g., three-way-catalyst (TWC) for gasoline engines and/or diesel oxidation catalyst (DOC) in the case of diesel engines), the sensor for continuous monitoring of residual HCs concentrations is strongly demanded to settle downstream of the treatment systems.

So far, there have been numerous reports in regard to solid electrolyte-based sensors [1,2], such as potentiometric (including mixed-potential-type) [3–20], amperometric [21–24] and impedancemetric [25–27] sensors, aiming at detection of HCs in various industrial and automotive fields. Among them, the sensors based on yttria-stabilized zirconia (YSZ) solid electrolyte seem to have a highly promising potential to detect HCs at rather high temperature and under very harsh conditions, because they have been already approved for the operation in real automotive exhaust to detect oxygen concentration (λ-sensor). Additionally, the amperometric zirconia-based NOx sensor has been developed for real practical application [28]. However, so far there have been no reports in regard to YSZ-based HCs sensor which can be operated in real automotive exhaust. This is because of the fact that real car exhaust is usually composed of a multi-component gas mixture containing a lot of different fractions of the saturated and unsaturated HCs [29], and, hence, it is significantly difficult to determine the concentration of each gas. Therefore the measurement of total concentration of various HCs would be a great advantage for a development of future on-board diagnosis (OBD) system.

Quite recently, we have reported that the mixed-potential-type YSZ-based sensor attached with $ZnCr_2O_4$-sensing electrode (SE) showed highly sensitive electromotive force (*emf*) response to each of non-methane HCs (NMHCs), such as C_2H_6, C_2H_4, C_3H_8, C_3H_6, C_3H_4, *n*-C_4H_{10}, *iso*-C_4H_8 and 1-C_4H_8, and negligible responses to

* Corresponding author. Tel.: +81 92 583 8852; fax: +81 92 583 8976.
E-mail address: miurano@astec.kyushu-u.ac.jp (N. Miura).
[1] Present address: Department of Materials Science, School of Chemistry, Madurai Kamaraj University, Madurai, Tamilnadu 625021, India.

0039-9140/$ – see front matter © 2011 Elsevier B.V. All rights reserved.
doi:10.1016/j.talanta.2011.04.024

other co-existing gases (CO, NO_x, H_2, and CH_4) at 550 °C even in the presence of 5 vol.% water vapor [30]. Furthermore, this sensor exhibited the good linearity between the sensitivity and the logarithm of total concentration of gas mixture containing the various volume ratios of 1-C_4H_8, C_3H_6 and C_2H_6 in the range of 90–950 ppmC [30]. The obtained promising results indicated that this sensor could be applied for a practical application to measure the total concentration of various HCs mixture in a real automotive exhaust. The above-mentioned good sensing characteristics are well known to be affected by a kind and morphology of SE material. In particular, some of the spinel-type oxides have been considered as suitable SE candidates for solid electrolyte-based gas sensors, as reported elsewhere [31–34].

In the present study, our efforts were focused on the stabilization of highly attractive HCs sensing characteristics for the YSZ-based sensor using $ZnCr_2O_4$-SE over a long period of time. The addition of intermediate YSZ layer between $ZnCr_2O_4$-SE and a YSZ tubular solid electrolyte was found to be very functional in order to stabilize the sensor's response for about one month examined. The detailed characterization of the laminated ($ZnCr_2O_4$/YSZ)-SE and the HCs gas-sensing characteristics obtained for the YSZ-based attached with the laminated ($ZnCr_2O_4$/YSZ)-SE are reported and discussed here.

2. Experimental

2.1. Fabrication of sensing devices

A commercially available one-end-opened YSZ-tube (8 mol.% Y_2O_3 doped, Nikkato Corp., Japan) was used for the fabrication of a sensor device. The physical dimensions of the YSZ tube were 300 mm in length and 5 and 8 mm in inner and outer diameters, respectively. Each of the commercial oxide powders ($ZnCr_2O_4$ [Kojundo Chemical Lab. Co., Ltd., Japan] and YSZ [Tosoh Co. Ltd., Japan]) or their mixture were thoroughly mixed with α-terpineol, and the resulting pastes were applied on the outer surface of the YSZ tube to form SE. In all cases, the width of the painted area for a belt-like SE was about 3 mm. The thickness of SE was estimated to be about 30 μm. A commercial Pt paste was applied on the top of the inner and outer surface of the YSZ tube to fabricate reference electrode (RE) and counter electrode (CE), respectively. The YSZ tube coated with the oxide and Pt pastes was dried in an oven at 130 °C overnight and sintered at 1100 °C for 2 h in air. In this study, three different structures of SE were fabricated: (a) the single $ZnCr_2O_4$-SE, (b) the composite ($ZnCr_2O_4$ + 10 wt% YSZ)-SE [thereinafter, ($ZnCr_2O_4$ + YSZ)-SE], and (c) the laminated ($ZnCr_2O_4$/YSZ)-SE. Fig. 1 shows the schematic views (a–c) of the fabricated SEs and the sketch (d) of the YSZ-based sensor used for the evaluation of gas-sensing properties.

2.2. Evaluation of sensing characteristics

The gas sensing characteristics of the fabricated sensors were evaluated in a conventional gas-flow apparatus equipped with an electric furnace operated at 550 °C. The sample gas containing each of various target gases were prepared by diluting each parent gas with the base air (dry synthetic air + 5 vol.% water vapor). The water vapor was introduced into the measuring system along with the base gas or the sample gas by using a water-vapor generator coupled with a small evaporator and a micro-flow pump (Hitachi L-2100, Japan). Each concentration of NO_2 and reducing gases (CO, NO, H_2, HCs) was always set to 100 ppm. The concentration of C_3H_6 was varied from 20 to 800 ppm as a representative HCs. The influence of each of co-existing gases, such as H_2O (0–10.8 vol.%), O_2 (2–20 vol.%), and CO_2 (0–20 vol.%) was also investigated. The total

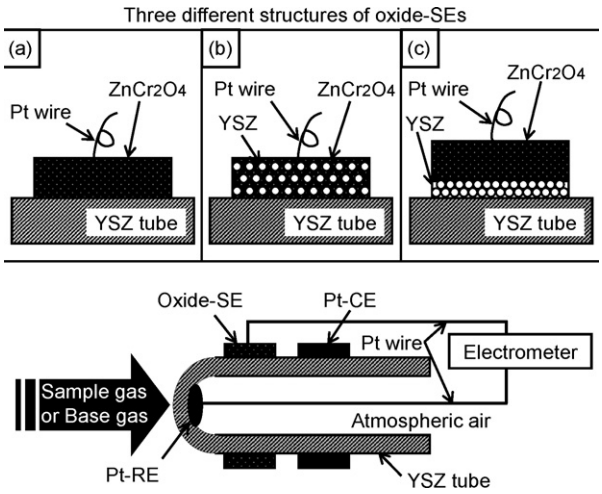

Fig. 1. Schematic view of oxide-based SE structure for (a) the single $ZnCr_2O_4$-SE, (b) the composite ($ZnCr_2O_4$+YSZ)-SE and (c) the laminated ($ZnCr_2O_4$/YSZ)-SE. (d) Sketch of the tubular YSZ-based sensor attached with outer oxide-based SE, outer Pt-CE and the inner Pt-RE.

flow-rate of the base gas as well as the sample gas was fixed at 100 cm^3 min^{-1}. The difference in *emf* between SE and the inner Pt-RE, exposed always to the atmospheric air, of the tubular sensor was measured with a digital electrometer (Advantest, R8240) as a sensing signal. The *emf* between SE and the outer Pt-CE was measured in the oxygen concentration dependency test. The gas sensitivity (Δemf) was defined as the difference between *emf* value in the sample gas and that in the base gas.

The current–voltage (polarization) curves were measured by potentiodynamic method at a constant scan-rate of 2 mV min^{-1} by using an automatic polarization system (HZ-3000, Hokuto Denko, Japan). The AC complex-impedance measurements for the tubular YSZ-based sensor were performed by means of an impedance analyzer (1255WB, Solartron, UK) in the frequency range of 0.1 Hz to 1 MHz, when SE was exposed to 100 ppm C_3H_6. The amplitude of AC potential signal and the applied DC potential were fixed at 50 mV and 0 mV, respectively, during all measurements.

2.3. Characterization of SE material

Crystal structures of the fabricated SEs were determined by X-ray diffraction (XRD, RINT 2100VLR/PC, Rigaku, Japan) analysis using Cu Kα radiation (40 kV, 20 mA) at a scan speed of 1° min^{-1}. Morphologies of SEs were observed by a field-emission scanning electron microscope (FE-SEM, JSM-6340F, JEOL, Japan). Because of the large physical dimensions of the tubular YSZ-based sensors examined in the present study, XRD and SEM observations were carried out on the SEs fabricated on YSZ plate (10 × 10 mm in square and 0.2 mm in thickness).

3. Results and discussion

3.1. Comparison of sensing characteristics for the different SEs

Initially, the stability of sensitivity to 100 ppm C_3H_6 for each of the fabricated sensors was examined when each sensor was operated at 550 °C in the presence of 5 vol.% H_2O for about a month. The obtained results are depicted in Fig. 2. It is seen that the C_3H_6 sensitivity of the sensor using the single $ZnCr_2O_4$-SE was found to be stable only for 10 days (Fig. 2(a)). The examination of responses against 100 ppm C_3H_6 and NO_2 measured at the 2nd and 23rd day of operation (shown in an inset of Fig. 2(a)) indicated tremendous change not only in the absolute *emf* value

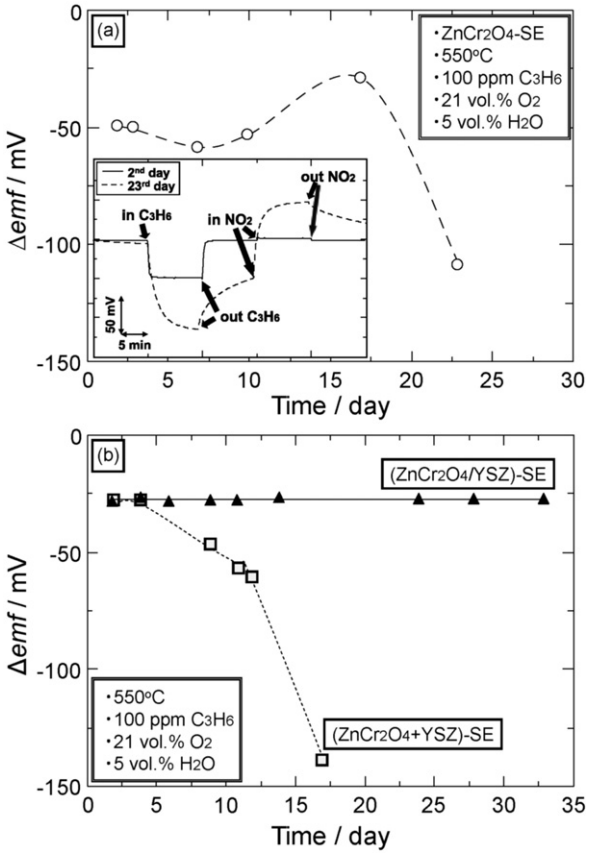

Fig. 2. Time course of C_3H_6 sensitivities at 550 °C under the wet condition (5 vol.% H_2O) for the sensor attached with each of (a) the single $ZnCr_2O_4$-, and (b) the composite ($ZnCr_2O_4$+YSZ)- and (c) laminated ($ZnCr_2O_4$/YSZ)-SEs. (Inset of (a): comparison of response transients to 100 ppm C_3H_6 and NO_2 at the 2nd and 23rd day of sensor's operation).

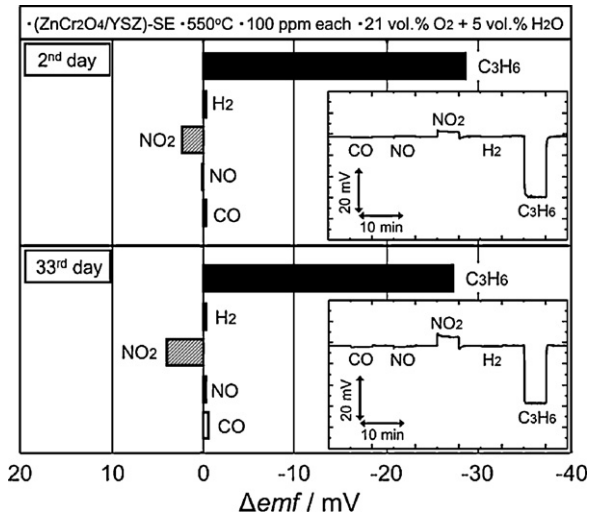

Fig. 3. Comparison of cross sensitivities and response transients to various gases at 550 °C in the presence of 5 vol.% H_2O for the sensor using the laminated ($ZnCr_2O_4$/YSZ)-SE at the 2nd and 33rd day of operation.

but also in response/recovery rate which became much slower. The C_3H_6 sensitivity for the sensor attached with the composite ($ZnCr_2O_4$ + YSZ)-SE (Fig. 2(b)) exhibited the similar behavior with that of the sensor using the single $ZnCr_2O_4$-SE, tended to increase drastically after about 10-day operation at 550 °C. On the contrary, the sensor attached with the laminated ($ZnCr_2O_4$/YSZ)-SE exhibited very stable sensitivity to 100 ppm C_3H_6 even after 30-day operation at 550 °C in the presence of 5 vol.% H_2O (Fig. 2(b)). In addition to providing the highly stable C_3H_6 sensitivity, the selectivity to C_3H_6 was not altered after one month operation at high temperature, as shown in Fig. 3. It is clearly seen that all main gas-sensing characteristics for the present sensor, i.e. the C_3H_6 sensitivity and selectivity, the minor responses to other co-existing gases (CO, NO_x and H_2) and fast response/recovery rate, observed at the 2nd and 33rd day of sensor's operation were quite similar to each other. Undoubtedly, the addition of intermediate YSZ layer between oxide and YSZ tube seems to be a very promising solution for stabilization of response for YSZ-based gas sensors.

To investigate the reasons for such a stabilization, both sensors using the single $ZnCr_2O_4$- and the laminated ($ZnCr_2O_4$/YSZ)-SEs were investigated by means of XRD, SEM and complex-impedance measurements. Firstly, XRD patterns (not shown here) were recorded for each of $ZnCr_2O_4$-SE and ($ZnCr_2O_4$/YSZ)-SE after (1) sintering at 1100 °C for 2 h and (2) operating at 550 °C for 23 days. All XRD patterns revealed the Bragg reflections, which were assigned to each of $ZnCr_2O_4$ [JCPDS no. 22-1107] and YSZ [JCPDS no. 48-0224] single phase. It could be therefore confirmed that both compounds remained their original crystal structure even after operating at 550 °C for 23 days. Furthermore, in the case of the laminated ($ZnCr_2O_4$/YSZ)-SE, the positions of Bragg reflections (θ) assigned to $ZnCr_2O_4$ were exactly matched with those for the standard $ZnCr_2O_4$. This indicates that there is no formation of solid solution between $ZnCr_2O_4$ and YSZ, and $ZnCr_2O_4$ seems to be chemically and thermally stable over a whole period of measurements.

Fig. 4 shows the representative cross-sectional SEM images of the single $ZnCr_2O_4$-SE and the laminated ($ZnCr_2O_4$/YSZ)-SE observed at the 1st and 23rd day of sensor's operation. Before coming into discussion of SEM observation, it is necessary to point out that the present YSZ-based HCs sensors are operating under the mixed-potential sensing mechanism. The mixed-potential arises by competing two electrochemical reactions at the interface between oxide-based SE and YSZ, which is pure oxygen-ion conducting solid electrolyte. Hence, in the case of single $ZnCr_2O_4$-SE, the interface is considered to be in between $ZrCr_2O_4$ grains and YSZ tube, whereas that for the laminated ($ZnCr_2O_4$/YSZ)-SE is in between $ZrCr_2O_4$ grains and YSZ powder. As seen from Fig. 4(a), comparison of the state of interface for the single $ZnCr_2O_4$-SE revealed slight agglomeration of $ZnCr_2O_4$ particles after 23-day operation. However, well-marked difference of the change in interface morphology at the interface was not seen, as also reported elsewhere [35]. The similar agglomeration was also observed for the laminated ($ZnCr_2O_4$/YSZ)-SE after its operation for 23 days at 550 °C (Fig. 4(b)). In this case, however, $ZnCr_2O_4$ grains were not located on flat and highly dense YSZ tube, but they were penetrating into the YSZ-powdered layer and buried by YSZ particles, as shown in Fig. 5. It is seen that, initially, the larger $ZnCr_2O_4$ grains (the upper part of Fig. 5(a)) are finely contacted with the smaller YSZ particles (the lower part of Fig. 5(a)), and then YSZ particles are tightly arranged on the YSZ plate (Fig. 5(b)). From these results, we could speculate that the stabilization of gas-sensing characteristics for the laminated ($ZnCr_2O_4$/YSZ)-SE might be driven by the stabilized $ZnCr_2O_4$ grains, which are buried in the layer of YSZ particles, in comparison with the unstable response of single $ZnCr_2O_4$-SE, where the $ZnCr_2O_4$ grains are just attached onto the dense YSZ tube.

In addition, the complex-impedance spectra (Nyquist plots) of the sensor using each of the single $ZnCr_2O_4$-SE (Fig. 6(a)) and the laminated ($ZnCr_2O_4$/YSZ)-SE (Fig. 6(b)) were measured in the sample gas containing 100 ppm C_3H_6 at 550 °C under the wet condition. At the 2nd day of operation, the resistance value of the laminated ($ZnCr_2O_4$/YSZ)-SE in real part (Z') at the frequency of 0.1 Hz is much smaller (around 10 kΩ) than that for the single $ZnCr_2O_4$-SE (around 50 kΩ). This means that the current value of the electrochemical

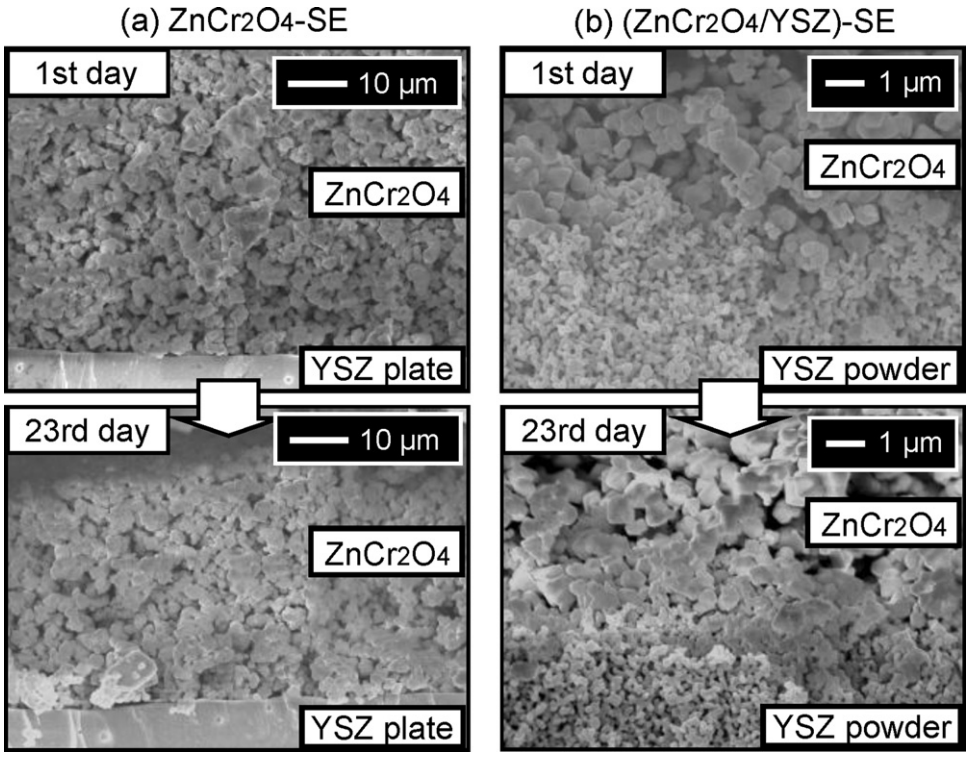

Fig. 4. Cross-sectional SEM images for the interface between YSZ tube and (a) the single $ZnCr_2O_4$-SE or (b) the laminated ($ZnCr_2O_4$/YSZ)-SE, at the 1st and 23rd day of sensor's operation at 550 °C.

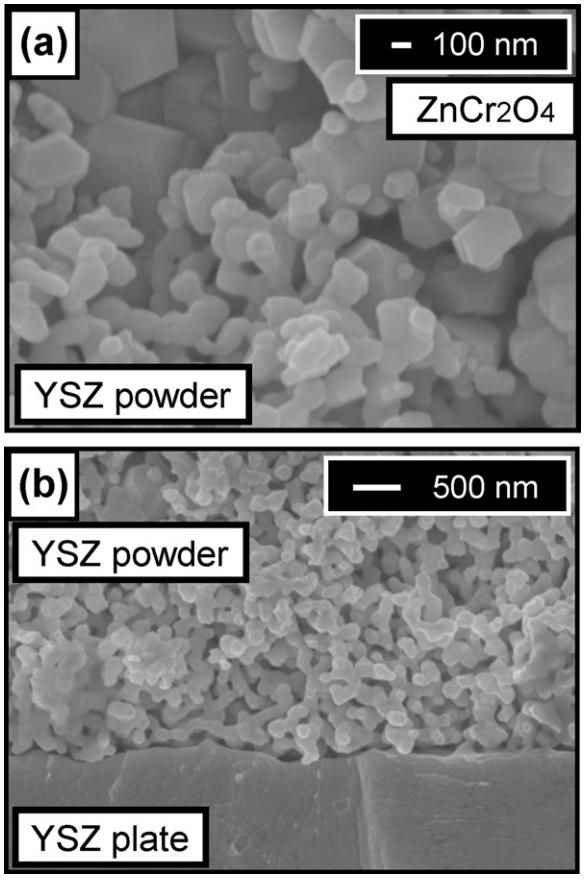

Fig. 5. Representative SEM images for (a) the interface between $ZnCr_2O_4$ grains and YSZ particles and for (b) that between YSZ particles and YSZ plate.

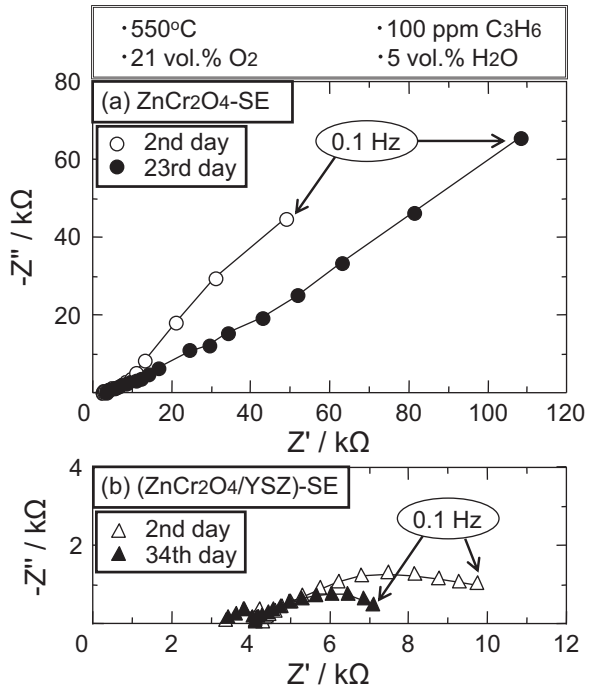

Fig. 6. Comparison of Nyquist plots in 100 ppm C_3H_6 at 550 °C under the wet condition for the sensors using (a) the single $ZnCr_2O_4$-SE and (b) the laminated ($ZnCr_2O_4$/YSZ)-SE, at the 2nd day of observation and after the long-term operation (the 23rd or 34th day).

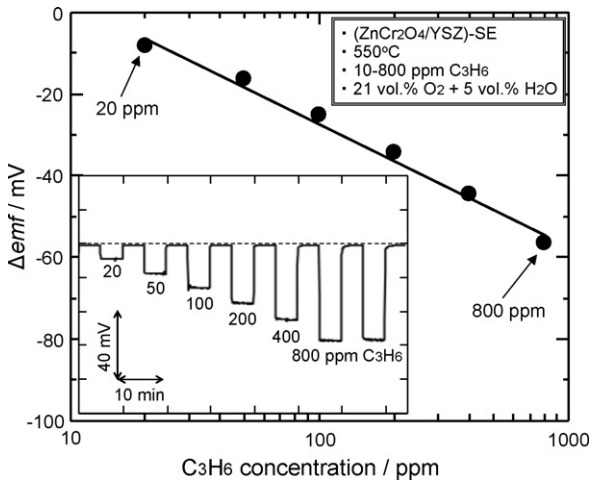

Fig. 7. Dependence of Δemf on the C_3H_6 concentration at 550 °C for the sensor attached with the laminated ($ZnCr_2O_4$/YSZ)-SE. (Inset: response transients to C_3H_6 in the concentration range of 20–800 ppm.)

reactions including O_2 or C_3H_6, occurring at the interface between SE and YSZ, was increased by about 5 times just by means of the addition of intermediate YSZ layer between $ZnCr_2O_4$-SE and YSZ tube. Such an increase in the current value was also confirmed by the polarization (I–V) curve measurement (not shown here). In other words, the number of reaction sites favored for the electrochemical reactions at the interface between $ZnCr_2O_4$ and YSZ layer was increased drastically. Moreover, the estimated resistance value at 0.1 Hz for the sensor using the single $ZnCr_2O_4$-SE was increased twofold after the sensor's operation of 23 days, while that for the sensor attached with the laminated ($ZnCr_2O_4$/YSZ)-SE was even decreased a bit after the operation of 34 days.

In general, the sensing characteristics of mixed-potential-type sensor are affected by both of the catalytic activity for gas-phase reaction in SE matrix and the catalytic activities for two competing electrochemical reactions at SE/YSZ interface [36]. Based on the present results, it can be speculated that the *emf* responses to gases are more influenced by the catalytic activities for the electrochemical reactions at the interface between $ZnCr_2O_4$ and YSZ rather than that for the gas-phase reaction, since only one kind of SE ($ZnCr_2O_4$) was used in the present study. Thus, the addition of secondary YSZ layer between $ZnCr_2O_4$-SE and YSZ tube seemed to stabilize the electrochemical reaction sites at the interface and resulted in much better stability of the present sensor. Such a method could be, therefore, considered as one of useful and general techniques for stabilization of gas-sensing characteristics for electrochemical YSZ-based gas sensors, including not only the mixed-potential-type sensors but also amperometric and impedancemetric ones, because, in all the above-mentioned sensors, the high response to a target gas is derived from the electrochemical reactions occurring at the interface between SE and YSZ solid electrolyte.

3.2. Performance of sensor using the laminated ($ZnCr_2O_4$/YSZ)-SE

After attaining stable C_3H_6 response, the gas-sensing characteristics of the mixed-potential-type YSZ-based sensor using the laminated ($ZnCr_2O_4$/YSZ)-SE were further examined at 550 °C under the wet condition. Fig. 7 shows the dependence of Δemf on the C_3H_6 concentration in the range of 20–800 ppm. The C_3H_6 sensitivity depended linearly on the logarithm of C_3H_6 concentration in the examined range. Such a linear dependence is usually a typical behavior for a mixed-potential-type sensor [36]. The response transients to each C_3H_6 concentration are given in an inset of Fig. 7. The response/recovery signal changed rapidly upon switching the sample or base gas and both 90% response and 90% recovery times were less than 10 s.

It should be emphasized that large amounts of CO_2 and water vapor are usually emitted from gasoline or diesel vehicle upon combustion of the gasoline or light gas oil fuels, respectively. The concentrations of these co-existing gases in automotive exhausts usually fluctuate drastically due to a change in internal-combustion engine conditions. Thus, it is of particular importance that the sensitivity of a sensor should not be affected by the change in concentrations of the co-existing gases mentioned above. The *emf* responses to the base gas, 100 and 400 ppm C_3H_6 were therefore recorded for the present sensor attached with the laminated ($ZnCr_2O_4$/YSZ)-SE at 550 °C when the concentration of water vapor was fixed at 5 vol.% and CO_2 concentration was varied from 0 to 20.0 vol.%. The obtained results are given in Table 1. It was observed that the *emf* responses to those gases were hardly affected by the change in CO_2 concentration. Then, the concentration of water vapor was also changed from 0 to 10.8 vol.%. The obtained *emf* responses were also not altered by the change in H_2O concentration, as shown in Table 2. This result assumes that water vapor molecules do not participate in the electrochemical reactions at the interface. Both these results are highly preferable for an actual application.

Apart from CO_2 and water vapor, the effect of change in O_2 concentration on gas sensitivity seems to be even much more important, because oxygen is directly involved in the response-generating electrochemical reactions at the SE/YSZ interface. Thus, the *emf* responses to base gas, 100 and 400 ppm C_3H_6 were measured by changing the O_2 concentration in the range of 2–20 vol.%. First, the effect of O_2 concentration on the *emf* response was examined for the tubular YSZ-based sensor using the outer ($ZnCr_2O_4$/YSZ)-SE and the inner Pt/air-RE (exposed always to the atmospheric air). As shown in Fig. 8(a), the *emf* responses negatively increased synchronously with decreasing O_2 concentration. It is well-known that, when SE is exposed to oxygen, the change in *emf* response is derived from the equilibrium electrochemical reaction of oxygen;

$$O_2 + 4e^- \leftrightarrows 2O^{2-} \quad (1)$$

and the change in *emf* response follows Nernst equation;

$$E = E^o + \frac{RT}{nF} \ln\left(\frac{P_{O_2}}{P'_{O_2}}\right) \quad (2)$$

In our case, based on the results obtained for the base gas, the number of electron (n) calculated by Eq. (2) was found to be close to 4. This indicates that the electrochemical equilibrium reaction (1) occurs under the present operating condition and the sensor is working as an oxygen concentration cell. In the case of sample gas composed of oxygen and 100 (or 400) ppm C_3H_6, the *emf* responses also negatively increased with decreasing O_2 concentration. It should be noted that the tendency of change in *emf* responses to 100 (or 400) ppm C_3H_6 was similar to that for the base gas. This means that the electrochemical reaction of C_3H_6 at the ($ZnCr_2O_4$/YSZ)-SE/YSZ interface might not be inhibited by decreasing/increasing O_2 concentration. To confirm this, the *emf* responses to the base gas, 100 and 400 ppm C_3H_6 for the planar-like sensor using the laminated ($ZnCr_2O_4$/YSZ)-SE and the outer Pt-CE were examined at 550 °C, when the O_2 concentration was also similarly varied from 2 to 20 vol.%. The planar-like sensor's configuration means that both of the laminated ($ZnCr_2O_4$/YSZ)-SE and the outer Pt-CE were exposed to the same gas condition. As a result, the *emf* responses to each of the examined gas compositions were hardly affected by the change in O_2 concentration, as shown in Fig. 8(b). These results indicate that the catalytic activity to the electrochemical equilibrium reaction of O_2 (1) for both of the lam-

Table 1
Comparison of *emf* responses to the base gas, 100 and 400 ppm C_3H_6 on the change in CO_2 concentration in the range of 0–20.0 vol.% at 550 °C for the sensor using the laminated ($ZnCr_2O_4$/YSZ)-SE.

Sensor response (mV)	CO2 concentration (vol.%)				
	0	5.0	10.0	15.0	20.0
Base gas (air)	0.4	0.26	0.14	0.03	−0.03
100 ppm C3H6	−35.4	−35.6	−35.8	−36.0	−36.3
400 ppm C3H6	−63.0	−63.7	−63.7	−64.1	−63.8

Table 2
Comparison of *emf* responses to the base gas, 100 and 400 ppm C_3H_6 on the change in H_2O vapor concentration in the range of 0–10.8 vol.% at 550 °C for the sensor using the laminated ($ZnCr_2O_4$/YSZ)-SE.

Sensor response (mV)	H2O vapor concentration (vol.%)							
	0 (dry)	2.70	4.05	5.40	6.75	8.10	9.45	10.8
Base gas (air)	−0.6	−0.9	−1.2	−1.5	−1.8	−2.0	−2.3	−2.6
100 ppm C3H6	−33.7	−32.2	−31.9	−32.2	−32.6	−32.5	−32.9	−32.9
400 ppm C3H6	−59.5	−57.2	−57.3	−58.2	−58.5	−58.7	−59.2	−59.5

inated ($ZnCr_2O_4$/YSZ)-SE and the outer Pt-CE/inner Pt-RE is nearly same each other.

We have recently reported that the mixed-potential-type YSZ-based sensor attached with the single $ZnCr_2O_4$-SE can measure the total concentration of various HCs in the mixture of three kinds of HCs, such as 1-C_4H_8, C_3H_6 and C_2H_6 [30]. Therefore, to check the behavior of the sensor used in the present study, the cross sensitivities to eight kinds of HCs and H_2 were examined and compared, as shown in Fig. 9. It is seen that Δemf varies almost linearly with the number of carbon in HC in the examined range of C_2–C_4 (see the inset of Fig. 9). More importantly, the present sensor gives almost same Δemf to HCs which have equal carbon numbers, irrespective of the chemical bonding nature (saturated or unsaturated) and spatial coordination of CH groups. These results were similar to those reported before for the sensor attached with the single $ZnCr_2O_4$-SE [30]. It is also suggested that the present sensor using the laminated ($ZnCr_2O_4$/YSZ)-SE could be applied for measurements of total concentration of various HCs. To substantiate this, three different HCs were mixed (mixture 1: 1-C_4H_8, C_3H_6 and C_2H_6; mixture 2: *n*-C_4H_{10}, C_3H_6, and C_2H_4) in various compositions (in volume ratio) and then the Δemf values against each gas mixture were recorded for the present sensor operated at 550 °C under the wet condition (5 vol.% water vapor). The definition of total concentration of various HCs (ppmC) has been previously mentioned in our paper [30]. Fig. 10 depicts the dependence of Δemf on the total concentration of various HCs mixtures for the present sensor at 550 °C in the presence of 5 vol.% H_2O. It is clearly seen that Δemf to various HCs mixtures containing different volume ratios of three kinds of HCs varies almost linearly with regard to the logarithm of total concentration of HCs (ppmC) in the examined range of 90–2600 ppmC. Thus, it is concluded that the present sensor could also detect successfully the total concentration of various HCs mixture and be

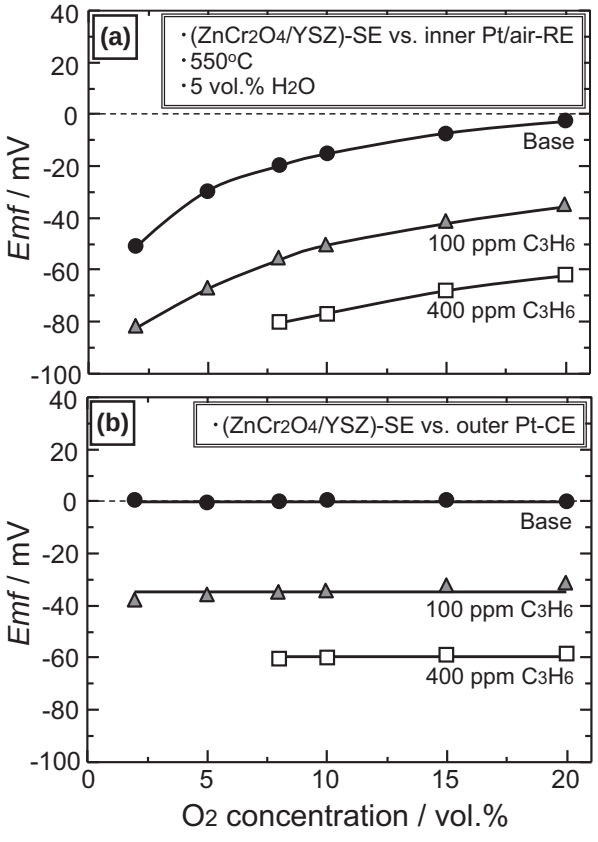

Fig. 8. Dependence of *emf* responses to the base gas, 100 and 400 ppm C_3H_6 on the change in O_2 concentration in the range of 2–20 vol.% at 550 °C under the wet condition for (a) the tubular-type sensor using the laminated ($ZnCr_2O_4$/YSZ)-SE and the inner Pt/air-RE, and (b) the planar-like sensor using the laminated ($ZnCr_2O_4$/YSZ)-SE and the outer Pt-CE.

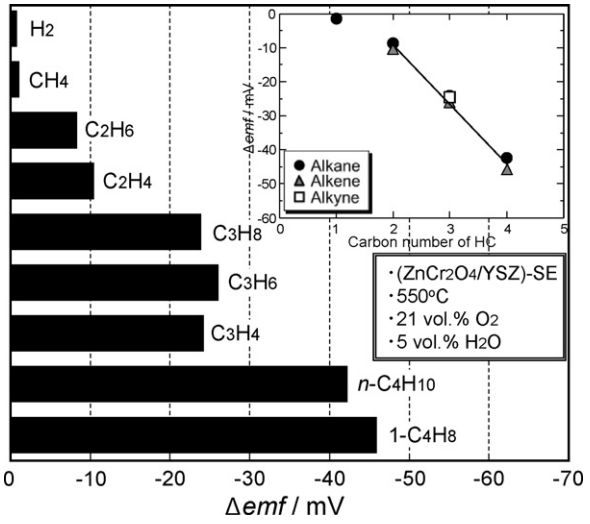

Fig. 9. Comparison of cross sensitivities to eight kinds of various HCs and H_2 (100 ppm each) at 550 °C under the wet condition (5 vol.% water vapor) for the sensor using the laminated ($ZnCr_2O_4$/YSZ)-SE. (Inset: dependence of sensitivity (Δemf) on carbon number.)

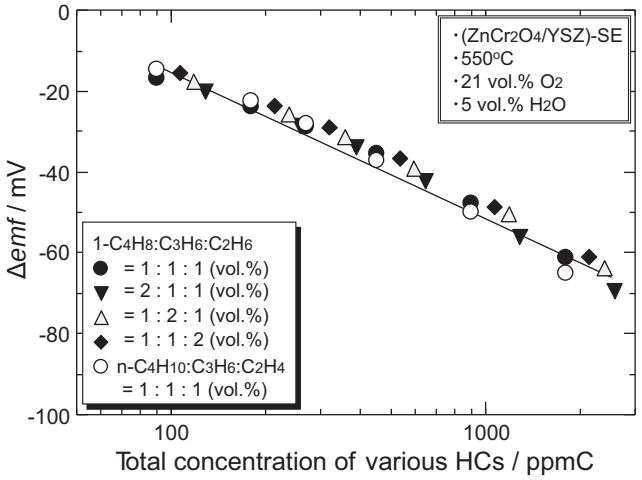

Fig. 10. Dependence of Δ*emf* on the total concentration of various HCs mixtures at 550 °C for the sensor attached with the laminated ($ZnCr_2O_4$/YSZ)-SE.

considered as one of possible candidates for the actual total HC sensor operating in automotive exhausts.

4. Conclusions

The improvement in stability of the gas-sensing characteristics for the mixed-potential-type YSZ-based sensor attached with single $ZnCr_2O_4$-SE was achieved by modification of SE structure with the addition of intermediate YSZ layer. The resulted tubular sensor consisted of the laminated ($ZnCr_2O_4$/YSZ)-SE and the inner Pt/air-RE was capable of providing highly stable HCs gas-sensing characteristics at 550 °C in the presence of 5 vol.% H_2O for more than one month examined. Based on the detailed SE characterization, the stabilization of gas response seemed to be caused by the stabilization of interface between the $ZnCr_2O_4$ grains worked as SE and the YSZ particles operated as oxygen-ion conducting solid electrolyte. In other words, the addition of intermediate YSZ layer improved the mechanical stabilization of interface by burying the as-fabricated $ZnCr_2O_4$ grains into the porous interlayer of YSZ particles. This results in stabilization of the electrochemical reaction sites at the interface between the laminated ($ZnCr_2O_4$/YSZ)-SE and YSZ solid electrolyte.

The fabricated sensor attached with the newly proposed laminated ($ZnCr_2O_4$/YSZ)-SE showed good linearity between Δ*emf* and the logarithm of the C_3H_6 concentration in the range of 20–800 ppm. The C_3H_6 sensitivity was hardly affected by the change in O_2, CO_2 and water vapor concentrations in the wide range. In addition, the sensor using the laminated ($ZnCr_2O_4$/YSZ)-SE gave almost same values of sensitivity to HCs that have equal carbon numbers (in the range of C_2–C_4); the response was irrespective of HCs chemical bonding nature as well as spatial coordination of CH groups. Furthermore, Δ*emf* varied almost linearly with the number of carbon in HC. Then, it was confirmed that the dependence of Δ*emf* to various HCs mixtures containing different volume ratios of three kinds of HCs exhibited good linearity with regard to the logarithm of total concentration of HCs in the examined range of 90–2600 ppmC. The obtained results seem to be promising in regard to a possible practical application of the present HCs sensor in real automotive exhaust.

Acknowledgements

This work was partially supported by "Grant-in-Aid for JSPS Fellows (No. 222597)", Kyushu University programs on "Novel Carbon Resource Sciences" and "Grant-in-Aid for Scientific Research (B) (No. 22350095)" from JSPS, Japan.

References

[1] J.W. Fergus, Sens. Actuator B: Chem. 122 (2007) 683–693.
[2] C.O. Park, J.W. Fergus, N. Miura, J. Park, A. Choi, Ionics 15 (2009) 261–284.
[3] T. Hibino, Y. Kuwahara, Y. Kuroki, T. Oshima, R. Inoue, S. Kitanoya, T. Fuma, Solid State Ionics 104 (1997) 163–166.
[4] N. Miura, T. Shiraishi, K. Shimanoe, N. Yamazoe, Electrochem. Commun. 2 (2000) 77–80.
[5] A. Hashimoto, T. Hibino, K. Mori, M. Sano, Sens. Actuator B: Chem. 81 (2001) 55–63.
[6] T. Hibino, A. Hashimoto, S. Kakimoto, M. Sano, J. Electrochem. Soc. 148 (1) (2001) H1–H5.
[7] B.K. Narayanan, S.A. Akbar, P.K. Dutta, Sens. Actuator B: Chem. 87 (2002) 480–486.
[8] J. Zosel, K. Ahlborn, R. Muller, D. Westphal, V. Vashook, U. Guth, Solid State Ionics 169 (2004) 115–119.
[9] J. Zosel, R. Müller, V. Vashook, U. Guth, Solid State Ionics 175 (2004) 531–533.
[10] G. Kyriakou, D.J. Davis, R.B. Grant, M.S. Tikhov, A. Keen, P. Pakianathan, R.M. Lambert, J. Phys. Chem. B 110 (2006) 24571–24576.
[11] T. Ueda, P. Elumalai, V.V. Plashnitsa, N. Miura, Chem. Lett. 37 (2008) 120.
[12] A. Dubbe, R. Moos, Sens. Actuator B: Chem. 130 (2008) 546–550.
[13] E.L. Brosha, R. Mukundan, F.H. Garzon, Electrochem. Solid-State Lett. 11 (2008) J92–J95.
[14] V.V. Plashnitsa, P. Elumalai, T. Kawaguchi, Y. Fujio, N. Miura, J. Phys. Chem. C 113 (2009) 7857–7862.
[15] L. Chevallier, S. Cordiner, E. Traversa, E.D. Bartolomeo, J. Electrochem. Soc. 156 (2009) J12–J15.
[16] P. Elumalai, V.V. Plashnitsa, Y. Fujio, N. Miura, Sens. Actuator B: Chem. 144 (2010) 215–219.
[17] Y. Fujio, V.V. Plashnitsa, N. Miura, J. Ceram. Soc. Jpn. 118 (3) (2010) 197–201.
[18] L. Chevallier, E. Traversa, E.D. Bartolomeo, J. Electrochem. Soc. 157 (11) (2010) J386–J391.
[19] T. Kida, H. Harano, T. Minami, S. Kishi, N. Morinaga, N. Yamazoe, K. Shimanoe, J. Phys. Chem. C 114 (2010) 15141–15148.
[20] M. Mori, Y. Sadaoka, Sens. Actuator B: Chem. 146 (2010) 46–52.
[21] A. Dutta, H. Nishiguchi, Y. Takita, T. Ishihara, Sens. Actuator B: Chem. 108 (2005) 368–373.
[22] T. Ueda, P. Elumalai, M. Nakatou, N. Miura, Electrochem. Commun. 9 (2007) 197–200.
[23] G. Kyriakou, A.V. Stevens, D.J. Davis, R.B. Grant, M.S. Tikhov, R.M. Lambert, J. Appl. Electrochem. 38 (2008) 1089–1096.
[24] Z. Bi, H. Matsumoto, T. Ishihara, Solid State Ionics 179 (2008) 1641–1644.
[25] M. Nakato, N. Miura, Sens. Actuator B: Chem. 120 (2006) 57–62.
[26] R. Wama, M. Utiyama, V.V. Plashnitsa, N. Miura, Electrochem. Commun. 9 (2007) 2774–2777.
[27] R. Wama, V.V. Plashnitsa, P. Elumalai, M. Utiyama, N. Miura, Solid State Ionics 181 (2010) 359–363.
[28] Y. Iuchi, N. Kihara, Readout HORIBA Tech. Rep. 15 (1997) 47–51.
[29] M. Han, D.N. Assanis, T.J. Jacobs, S.V. Bohac, J. Eng. Gas. Turb. Power: Trans. ASME 130 (2008) 042803-1–042803-10.
[30] Y. Fujio, V.V. Plashnitsa, P. Elumalai, N. Miura, Electrochem. Solid State Lett. 11 (10) (2008) J73–J75.
[31] N. Miura, H. Kurosawa, M. Hasei, G. Lu, N. Yamazoe, Solid State Ionics 86–88 (1996) 1069–1073.
[32] N. Miura, S. Zhuiykov, T. Ono, M. Hasei, N. Yamazoe, Sens. Actuator B: Chem. 83 (2002) 222–229.
[33] W. Xiong, G.M. Kale, Electrochem. Solid State Lett. 8 (6) (2005) H49–H53.
[34] W. Xiong, G.M. Kale, Anal. Chem. 79 (2007) 3561–3567.
[35] R. Wama, V.V. Plashnitsa, P. Elumalai, T. Kawaguchi, Y. Fujio, M. Utiyama, N. Miura, J. Electrochem. Soc. 156 (5) (2009) J102–J107.
[36] N. Miura, P. Elumalai, V.V. Plashnitsa, T. Ueda, R. Wama, M. Utiyama, in: E. Comini, G. Faglia, G. Sberveglieri (Eds.), Solid-State Electrochemical Gas Sensing, Solid State Gas Sensing, Springer Science+Business Media LCC, New York, 2009, pp. 181–207.